International Journal of Scientific Research in Modern Science and Technology
ISSN: 2583 -7605 (Online)
Volume 5 | Issue 4 | April 2026
Available online at: https://ijsrmst.com/
DOI: https://doi.org/10.59828/ijsrmst.v5i4.431

Network-Based Co-Resistance Analysis Across Six Foodborne Bacterial Pathogens: Hub Gene Identification, Horizontal Gene Transfer Potential, and Multi-Criteria Drug Target Prioritisation

Vaishnavi Tiwari[1], Shishir Tripathi[2]

[1]Department of Zoology, Shri Lal Bahadur Shastri Degree College, Gonda, Uttar Pradesh, India

[2]Assistant Professor, Department of Zoology, Shri Lal Bahadur Shastri Degree College, Gonda, Uttar Pradesh, India

[2]Corresponding E-mail Id: shishir8686@gmail.com

Abstract

Background: *Antimicrobial resistance (AMR) poses an escalating global health threat, with foodborne pathogens serving as critical vectors for multi-drug resistance (MDR) dissemination across the One Health continuum. Although individual resistance mechanisms have been extensively characterised, the systems-level architecture of cross-species AMR gene co-occurrence networks remains poorly defined.*

Methods: *A binary presence/absence matrix of 47 AMR genes spanning 11 drug classes was assembled from six priority foodborne pathogens that include Campylobacter jejuni, Enterococcus faecium, Escherichia coli, Listeria monocytogenes, Salmonella enterica, and Staphylococcus aureus based on a comprehensive primary literature synthesis. Jaccard similarity-based co-occurrence statistics with Bonferroni correction were applied to construct an undirected co-resistance network. Network topology metrics (degree, betweenness, closeness, and eigenvector centrality; composite hub score) were computed alongside pairwise horizontal gene transfer (HGT) potential scores. A four-component weighted algorithm incorporating hub score, pathogen breadth, chromosomal stability, and essentiality was applied for drug target prioritisation.*

Results: *The network comprised 47 nodes and 205 statistically significant co-occurrence edges (density = 0.190; average clustering coefficient = 0.727). Three hub genes aac6_ib_cr, acrAB, and blaSHV achieved maximal hub scores (0.238 each). The E. coli–S. enterica dyad exhibited the highest inter-species HGT potential (score = 0.692), sharing 18 mobile AMR genes including colistin resistance determinants (mcr1, mcr4) and extended-spectrum beta-lactamases. Drug target prioritisation ranked topoisomerase subunits parC and parE highest (composite score = 0.590), followed by gyrA (0.562), gyrB (0.557), and the efflux pump regulator acrAB (0.547).*

Conclusion: *Network-based AMR analysis identifies discrete hub genes and critical inter-species HGT axes that are obscured by species-centric approaches. The E. coli–S. enterica axis warrants priority One Health surveillance, and efflux pump inhibition combined with novel-binding-mode topoisomerase inhibitor development represents a network-informed therapeutic strategy with broad cross-pathogen applicability.*

Keywords: *antimicrobial resistance; co-resistance network; horizontal gene transfer; foodborne pathogens; drug target prioritisation; One Health; multi-drug resistance; network biology*

1. INTRODUCTION

Antimicrobial resistance has transitioned from a localised clinical concern to a global systemic crisis. The World Health Organization designated MDR organisms as a defining public health threat in 2014, and projections estimate up to ten million annual deaths attributable to drug-resistant infections by 2050 surpassing cancer as a

leading cause of mortality [1,2]. Foodborne pathogens occupy a uniquely strategic position in this crisis: they traverse the entire One Health continuum, circulating across agricultural, environmental, and human clinical compartments while transporting and exchanging resistance determinants at each interface [3].

Extensive mechanistic and epidemiological cataloguing of AMR in individual foodborne pathogens has been undertaken [4-6]. Urban-Chmiel et al. (2022) provided an authoritative synthesis of resistance mechanisms in six priority species which include *Campylobacter jejuni, Enterococcus faecium, Escherichia coli, Listeria monocytogenes, Salmonella enterica,* and *Staphylococcus aureus* spanning resistance gene inventories, phenotypic profiles, and epidemiological distributions [4]. Despite this depth of per-species knowledge, a critical analytical gap persists as no formal systems-level analysis has characterised how resistance genes co-occur, co-select, and are potentially co-transferred across this foodborne pathogen community as a structured network.

Co-resistance which is simultaneous carriage of determinants conferring resistance to two or more antibiotic classes is clinically well-recognised but network-analytically undercharacterised. Mobile genetic elements (MGEs), including conjugative plasmids, transposons, and integrons, co-transfer resistance gene cassettes en masse, generating non-random co-occurrence patterns that constrain and amplify MDR phenotype evolution [7,8]. Identifying hub genes offers substantially greater therapeutic leverage than targeting individual peripheral resistance genes.

The present in silico study addresses this gap by constructing a cross-species co-resistance gene network from published AMR gene repertoires of six major foodborne pathogens. The specific objectives were to: (i) construct a Jaccard similarity-based co-occurrence network of 47 AMR genes across six pathogens; (ii) identify hub genes and bridging nodes using comprehensive centrality metrics; (iii) quantify pairwise inter-species HGT potential; and (iv) apply a multi-criteria composite scoring algorithm to prioritise drug target candidates. The study explicitly adopts a systems biology perspective, treating the foodborne resistome as a structured network with identifiable vulnerabilities amenable to targeted therapeutic intervention.

2. MATERIALS AND METHODS

2.1 Data Source and Pathogen Selection

All AMR gene data were sourced from Urban-Chmiel et al. (2022) [4], supplemented by primary literature cited therein. Six foodborne pathogens were selected based on global clinical relevance and documented resistance gene depth: *C. jejuni* (poultry-associated zoonotic pathogen), *E. faecium* (nosocomial Gram-positive; ESKAPE group), *E. coli* (ubiquitous MDR Gram-negative reservoir), *L. monocytogenes* (high case-fatality food safety pathogen), *S. enterica* (leading foodborne Gram-negative), and *S. aureus* (Gram-positive with community and healthcare phenotypes).

2.2 Presence/Absence Matrix Construction

A binary presence/absence (P/A) matrix was constructed with pathogens as rows and 47 AMR genes as columns, spanning 11 drug classes: aminoglycosides, beta-lactams, fluoroquinolones, glycopeptides, macrolide-lincosamide-streptogramins (MLS), multidrug efflux, oxazolidinones, phenicols, polymyxins, sulfonamides, and tetracyclines. A cell received the value 1 if the resistance gene was documented for the respective pathogen and 0 otherwise, yielding the primary analytical dataset.

2.3 Co-Occurrence Network Construction

For each gene pair, co-occurrence was quantified using the Jaccard similarity index ($J = |A \cap B| / |A \cup B|$, where A and B denote pathogen sets harbouring each gene). Statistical significance was evaluated using a hypergeometric test with Bonferroni correction for multiple comparisons (significance threshold: $p < 0.05$). Significant gene pairs were retained as edges in an undirected co-resistance network. Per-node topology metrics

were computed: degree centrality, betweenness centrality, closeness centrality, eigenvector centrality, and a composite hub score derived from the normalised sum of these four metrics. Analyses were performed in Python 3.10 using NetworkX 3.0, SciPy 1.10, and Pandas 2.0.

2.4 Horizontal Gene Transfer Potential Scoring

Inter-species HGT potential was estimated for all 15 pairwise pathogen combinations using a composite score incorporating: (i) the count of shared AMR genes between the two pathogens; (ii) the fraction of shared genes classified as mobile (plasmid-borne, transposon-associated, or integron-located); and (iii) a phylogenetic weighting factor reflecting known inter-species genetic exchange frequency. The resulting HGT potential score ranges from 0 (no estimated transfer risk) to 1 (maximum transfer risk).

2.5 Drug Target Prioritisation

Drug target candidates were ranked using a four-component composite priority score with the following weighted components: (i) hub score (weight: 0.25), normalised across all 47 genes; (ii) pathogen breadth (weight: 0.30), normalised to the maximum observed; (iii) chromosomal stability bonus (weight: 0.20), with values of 1.0 for chromosomally encoded genes and 0.5 for plasmid-borne genes; and (iv) literature-derived essentiality score reflecting functional indispensability of the gene product (weight: 0.25).

3. RESULTS

3.1 AMR Gene Presence/Absence Patterns

The binary P/A matrix revealed highly heterogeneous resistance gene distributions across the six pathogens (Figure 1). *E. coli* harboured the broadest resistance portfolio (26/47 genes; all 11 drug classes), followed by *S. enterica* (24 genes) and *E. faecium* (22 genes). *E. faecium* was distinguished by the breadth of Gram-positive-specific mechanisms, encompassing the complete vancomycin resistance loci (vanA, vanB, vanC) and multiple erm-family macrolide methylase genes. *C. jejuni* and *L. monocytogenes* exhibited the most restricted profiles (11 and 9 genes, respectively), consistent with their narrower ecological niches and intrinsic resistance architectures. *S. aureus* presented a distinctive profile characterised by mecA/mecC (methicillin resistance), multiple tetracycline efflux genes (tetK, tetL), and cfr/cfr_lin oxazolidinone resistance loci of particular clinical relevance given the last-resort status of linezolid.

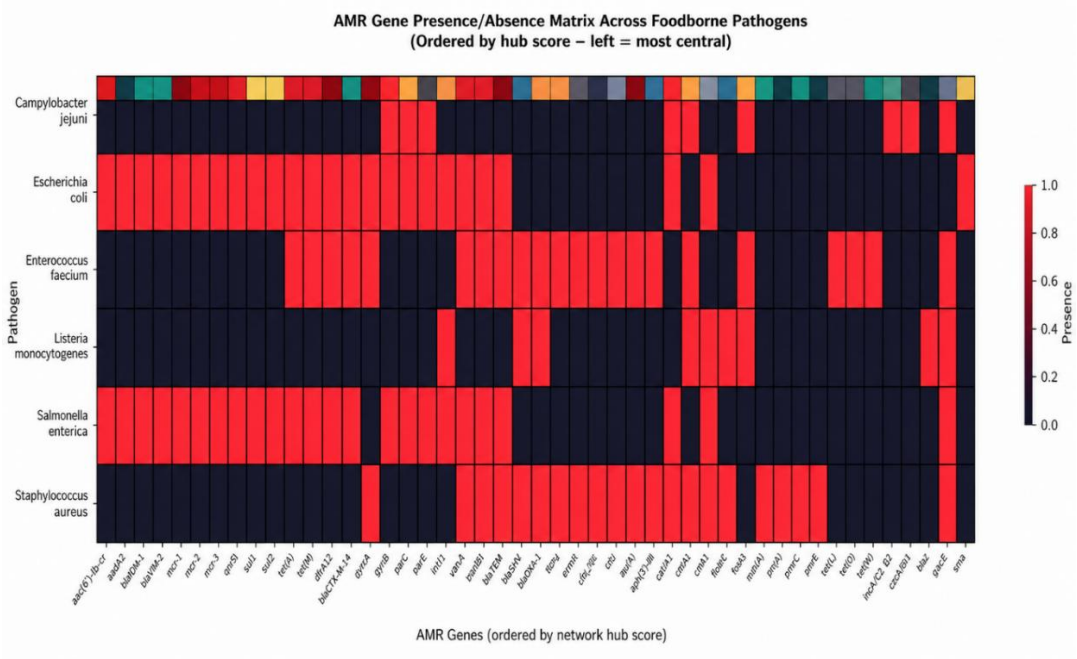

Figure 1. Presence/absence heatmap of 47 AMR genes across six foodborne pathogens. Columns are ordered by composite hub score (left = most central). Rows represent pathogens; gene presence is indicated (red); absence is dark. Drug class groupings are indicated on the x-axis. E. coli and S. enterica display the densest resistance portfolios.

3.2 Co-Resistance Network Topology and Hub Gene Identification

The co-resistance network comprised 47 nodes and 205 statistically significant co-occurrence edges (network density = 0.190; average clustering coefficient = 0.727; seven connected components). The high clustering coefficient indicates that co-occurring gene pairs form tightly interconnected modules, consistent with co-selection driven by shared MGE carriage rather than independent gene acquisition (Figure 2).

Three genes achieved the highest composite hub scores (0.238 each): aac6_ib_cr (fluoroquinolone/aminoglycoside bifunctional inactivation enzyme; plasmid-borne), acrAB (chromosomally encoded RND-family multidrug efflux pump; present in *E. coli* and *S. enterica*), and blaSHV (extended-spectrum beta-lactamase; plasmid-borne). Each hub gene co-occurred significantly with a minimum of 17 other resistance genes spanning multiple drug classes, identifying them as archetypal drivers of MDR co-selection. The chromosomal encoding of acrAB is particularly noteworthy: its hub status reflects a constitutive structural feature of the *E. coli/S. enterica* resistome that cannot be disrupted by plasmid-curing strategies, necessitating direct enzymatic inhibition as a therapeutic approach.

Betweenness centrality analysis identified aph3 (betweenness = 0.244) and the qnrA/qnrS quinolone resistance gene family (betweenness = 0.058) as key inter-modular bridging nodes (Figure 3). The qnr family, mediating target protection rather than enzymatic inactivation, was detected across E. coli, S. enterica, and E. faecium, spanning the principal Gram-negative/Gram-positive ecological divide in the dataset. Their high betweenness centrality implicates them as cross-phylum conduits for co-selection of otherwise unrelated resistance determinants.

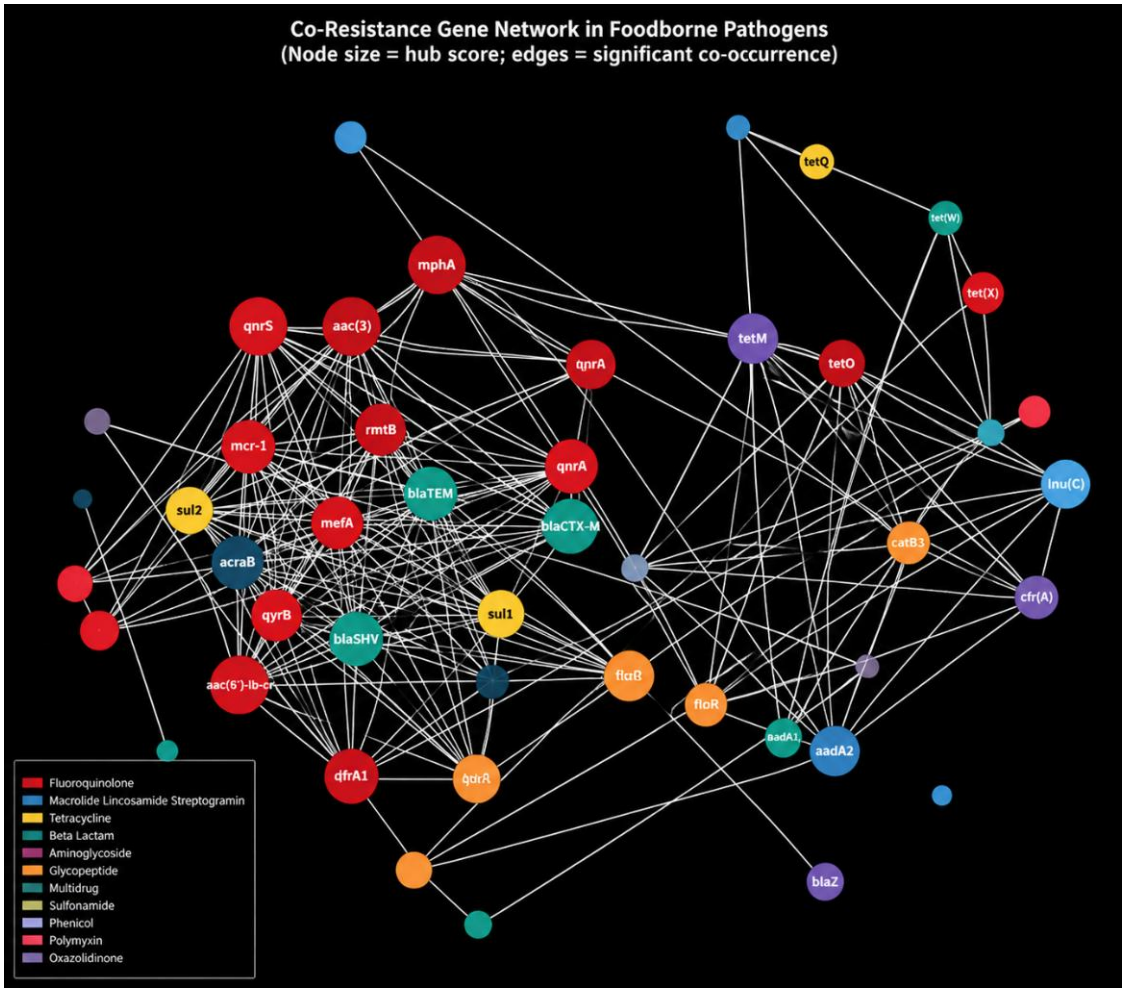

Figure 2. Co-resistance gene network across six foodborne pathogens. Node size is proportional to composite hub score; edge presence denotes statistically significant co-occurrence (Jaccard similarity; Bonferroni-corrected $p < 0.05$). Node colour indicates drug class. The central densely connected cluster is dominated by beta-lactam, fluoroquinolone, aminoglycoside, and polymyxin resistance genes, reflecting convergent co-selection on conjugative plasmid backbones.

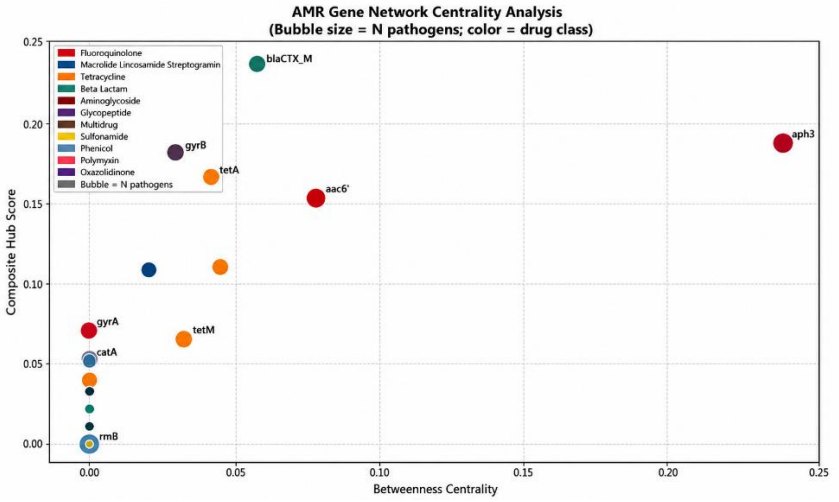

Figure 3. Bubble chart of composite hub score versus betweenness centrality for all 47 AMR genes. Bubble size indicates the number of pathogens harbouring each gene. Genes in the upper-right quadrant simultaneously exhibit high connectivity and high network bridging capacity, representing the highest-priority targets for therapeutic intervention.

3.3 Cross-Species HGT Potential

Pairwise HGT potential scores spanned a wide range from 0.063 (*E. coli–L. monocytogenes*) to 0.692 (*E. coli–S. enterica*), revealing a highly non-uniform inter-species resistance gene exchange landscape (Figure 4). The *E. coli–S. enterica* dyad was identified as the highest-risk pair, sharing 23 AMR genes of which 18 are classified as mobile (HGT potential score: 0.692). The shared mobile gene pool includes a clinically alarming combination of colistin resistance determinants (mcr1, mcr4), extended-spectrum beta-lactamases (blaCTX_M, blaSHV, blaTEM), pan-aminoglycoside resistance methylase (rmtB), Class 1 integrase (intI1), and plasmid-mediated quinolone resistance genes (qnrA, qnrB, qnrS).

The *E. faecium–S. aureus* dyad constituted the second highest inter-species risk pair (score: 0.414; 14 shared genes; 12 mobile), reflecting documented genetic exchange between these Gram-positive commensal and opportunistic pathogens in hospital and livestock environments. The shared mobile gene set includes vanA (high-level vancomycin resistance), cfr and cfr_lin (linezolid and multi-class resistance), and multiple macrolide resistance determinants, a cluster of last-resort antibiotic resistance genes with profound clinical implications.

Several lower-scoring pairs nonetheless carry significant One Health relevance. The *C. jejuni–L. monocytogenes* pair (score: 0.200) shares three exclusively mobile genes (ermB, tetM, tetO), and the intI1 Class 1 integrase gene, a master regulator of gene cassette capture is shared across *C. jejuni, E. coli,* and *S. enterica*, dramatically amplifying the effective scope of resistance gene flux in food chain environments.

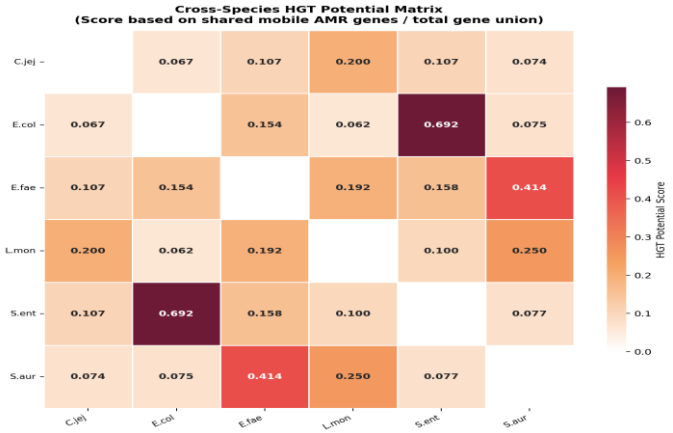

Figure 4. Cross-species HGT potential matrix across all 15 pairwise pathogen combinations. Colour intensity reflects the composite HGT potential score (range 0–1). The E. coli–S. enterica dyad (score = 0.692) dominates, followed by E. faecium–S. aureus (0.414), reflecting phylogenetic proximity and shared ecological habitats. The asymmetric distribution of scores underscores the non-random architecture of inter-species resistance gene exchange.

3.4 Drug Target Prioritisation

Multi-criteria composite scoring identified DNA gyrase and topoisomerase IV subunit genes as the highest-priority targets (Figure 5; Table 1). parC and parE, encoding topoisomerase IV subunits A and B, achieved joint top scores of 0.590, driven by breadth of pathogen coverage (*E. faecium, E. coli, S. enterica, S. aureus*), chromosomal location, and an essentiality score of 0.85. gyrA ranked third (score: 0.562; present in *C. jejuni, E. coli, S. enterica, S. aureus*) and gyrB fourth (score: 0.557; three pathogens).

The multidrug efflux pump acrAB ranked fifth (score: 0.547), uniquely occupying this position by virtue of its maximal hub score (0.238) and chromosomal stability, despite its narrower pathogen breadth (*E. coli* and *S. enterica* only). It is the sole non-fluoroquinolone target in the top five, underlining the disproportionate contribution of efflux pump-mediated resistance to MDR phenotypes in Gram-negative foodborne pathogens (Figure 5).

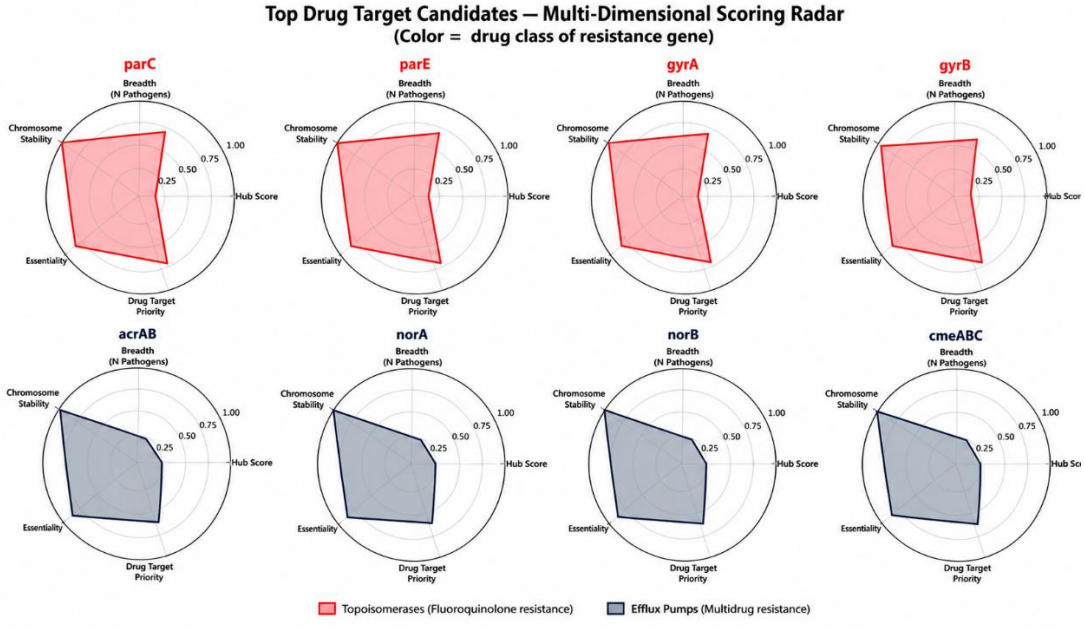

Figure 5. Multi-metric radar plots for the top ten drug target candidates. Each axis represents one scoring dimension: composite hub score, pathogen breadth (number of pathogens), chromosomal stability, and literature-derived essentiality. Genes occupying a large polygon area across all four axes — notably parC, parE, gyrA, gyrB — represent the most compelling multi-target therapeutic candidates.

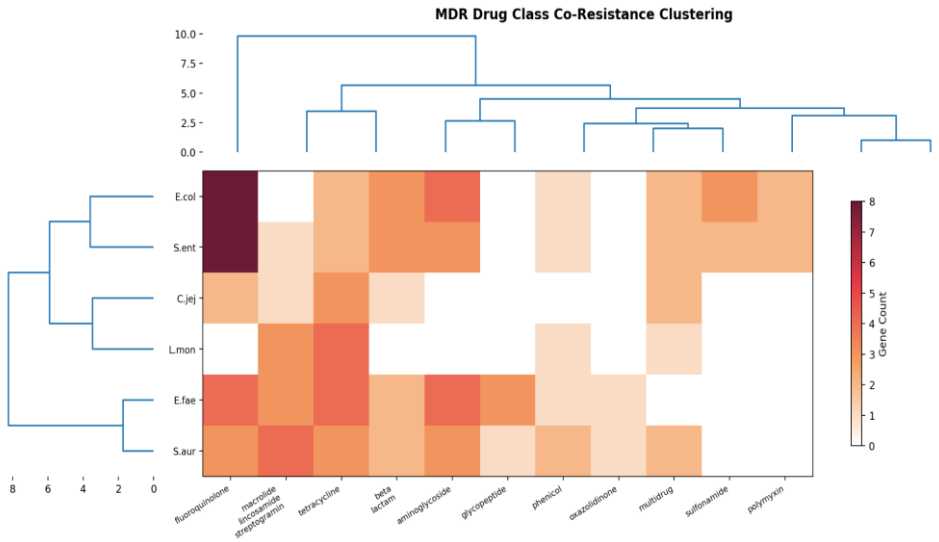

Figure 6. Hierarchical MDR drug-class co-resistance clustering heatmap, generated by unsupervised hierarchical clustering of pathogens and drug classes based on AMR gene co-occurrence. Two major clusters are evident: a Gram-negative cluster (E. coli, S. enterica, C. jejuni) dominated by fluoroquinolone, beta-lactam, and aminoglycoside resistance; and a Gram-positive cluster (S. aureus, E. faecium, L. monocytogenes) characterised by macrolide, glycopeptide, and cell-wall-targeting resistance genes.

Table 1. Top 10 Drug Target Candidates Ranked by Composite Priority Score

Rank	Gene	Drug Class	Pathogens (n)	Chromosomal	Priority Score	Key Pathogen(s)
1	parC	Fluoroquinolone	4	Yes	0.590	E. coli, S. enterica, E. faecium, S. aureus
2	Pare	Fluoroquinolone	4	Yes	0.590	E. coli, S. enterica, E. faecium, S. aureus
3	gyrA	Fluoroquinolone	4	Yes	0.562	C. jejuni, E. coli, S. enterica, S. aureus
4	gyrB	Fluoroquinolone	3	Yes	0.557	E. coli, S. enterica, S. aureus
5	acrAB	Multidrug efflux	2	Yes	0.547	E. coli, S. enterica
6	norA	Multidrug efflux	1	Yes	0.433	S. aureus
7	norB	Multidrug efflux	1	Yes	0.433	S. aureus
8	cmeABC	Multidrug efflux	1	Yes	0.426	C. jejuni
9	Lde	Multidrug efflux	1	Yes	0.422	L. monocytogenes
10	mecA	Beta-lactam	1	Yes	0.413	S. aureus

Composite priority score = weighted sum of hub score (0.25), pathogen breadth (0.30), chromosomal stability (0.20), and essentiality (0.25). Chromosomal: Yes = full stability weight.

4. DISCUSSION

4.1 Hub Genes as Mechanistic Drivers of MDR Co-Selection

The identification of aac6_ib_cr, acrAB, and blaSHV as top hub genes provides mechanistic insight into the structural basis of co-resistance architecture in foodborne pathogens. The bifunctional enzyme AAC(6′)-Ib-cr is uniquely significant as one of the few characterised resistance proteins spanning two mechanistically distinct antibiotic classes: it acetylates aminoglycosides at the 6′-amino position and simultaneously acetylates the piperazinyl nitrogen of fluoroquinolones (ciprofloxacin, norfloxacin), generating cross-class resistance from a single gene [9]. Its hub score of 0.238 directly reflects this cross-class co-selection capacity: any conjugative element carrying aac6_ib_cr is likely to co-harbour additional resistance cassettes, rendering the transfer event instantly polypharmacic.

The AcrAB-TolC efflux system, encoded by the chromosomal acrAB operon in E. coli and S. enterica, is the archetypal resistance-nodulation-division (RND) family efflux system with a substrate range spanning beta-lactams, fluoroquinolones, tetracyclines, macrolides, chloramphenicol, and bile salts [10]. Its overexpression, driven by regulatory mutations in marA, soxS, or acrR, is a common mechanism for simultaneous multi-class resistance elevation without new gene acquisition and, critically, without a new HGT event. The chromosomal encoding of acrAB means its hub status is irreversible by plasmid-curing strategies; efflux pump inhibitors (EPIs) targeting this system would simultaneously collapse co-resistance to five or more antibiotic classes, representing the archetypal example of network-informed leverage.

The ESBL gene blaSHV achieves high hub status through its consistent co-location on conjugative IncF and IncI plasmids that co-carry aminoglycoside (aac6), sulfonamide (sul1, sul2), and quinolone resistance determinants [11]. This plasmid architecture transforms blaSHV from a single resistance gene into a co-resistance cassette anchor, multiplying the phenotypic consequence of any single conjugative transfer event.

4.2 The E. coli–Salmonella HGT Axis: Priority One Health Surveillance Target

The *E. coli–S. enterica* HGT potential score of 0.692 is the highest in the dataset and is consistent with an extensive primary literature documenting conjugative plasmid exchange between these species in livestock environments, food processing facilities, and the human gastrointestinal tract [4,7]. Both species colonise intestinal niches of agricultural animals and humans simultaneously, share multiple plasmid incompatibility groups (IncF, IncI, IncN), and are continuously exposed to antibiotic selective pressure from therapeutic and prophylactic use in livestock production.

The co-occurrence of mcr1 and mcr4 (colistin resistance) with blaCTX_M (ESBL) and rmtB (pan-aminoglycoside 16S rRNA methylase) on shared mobile elements in both species is clinically alarming. Colistin is a last-resort polymyxin antibiotic used when carbapenem resistance forecloses standard options; the mobilisation of colistin resistance (mcr) onto plasmids already carrying ESBLs and aminoglycoside resistance creates combinations for which no reliable clinical antibiotic options remain [12]. Intensified monitoring of conjugative plasmid sharing between E. coli and S. enterica in food animal production and processing environments is urgently warranted and should be considered a One Health surveillance priority.

The *E. faecium–S. aureus* dyad (HGT score: 0.414) represents an independent Gram-positive risk axis of comparable clinical severity. The capacity of the vanA transposon (Tn1546) to transfer from *E. faecium* to *S. aureus* generates vancomycin-resistant MRSA (VRSA), widely considered one of the most feared AMR scenarios in clinical microbiology [4]. The additional sharing of cfr, conferring PhLOPSA-class resistance including linezolid, between these species in livestock and hospital settings threatens the last residual therapeutic options for invasive Gram-positive infections.

4.3 Fluoroquinolone Resistance as the Dominant Network Architecture

The dominance of fluoroquinolone resistance genes i.e. parC, parE, gyrA, gyrB in both network centrality and drug target rankings reflects the profound selective pressure that widespread clinical and veterinary fluoroquinolone use has exerted on foodborne pathogen populations. Critically, these topoisomerase target genes are not merely prevalent across pathogens: the hierarchical clustering heatmap (Figure 6) and network topology analysis together demonstrate that fluoroquinolone resistance is structurally central, co-occurring with resistance genes from at least seven other drug classes. This implies that selection of fluoroquinolone resistance simultaneously co-selects for broad MDR phenotypes, a phenomenon with direct implications for stewardship programmes that employ fluoroquinolone restriction as a resistance control measure.

The clinical implication is paradoxical: restricting fluoroquinolone use may partially dismantle co-resistance co-selection in Gram-negative foodborne pathogens, but the chromosomally fixed nature of gyrA/parC mutations in *C. jejuni*, which confer a fitness advantage even in the absence of antibiotic exposure severely limits the reversibility of fluoroquinolone resistance in this species regardless of usage patterns [4].

4.4 Network-Informed Drug Target Strategy

The composite prioritisation algorithm deliberately weights pathogen breadth alongside network centrality because a target essential in only one species, however critical, has narrower clinical utility than one essential across multiple pathogens. This framework identifies parC and parE as pre-eminent candidates: both are indispensable for bacterial DNA replication, chromosomally encoded, and shared across four of the six pathogens studied. Existing fluoroquinolones target these proteins, but pre-existing resistance mediated by parC/gyrA mutations combined with efflux overexpression has significantly eroded their clinical utility. The data therefore argue not for next-generation fluoroquinolones, which face pre-existing cross-resistance but for topoisomerase inhibitors with

novel binding modes (non-fluoroquinolone topoisomerase inhibitors; NFTIs) that are unaffected by existing QRDR mutations [13].

The ranking of acrAB at position five, despite its restricted pathogen breadth, reflects a critical network-level insight: an EPI disrupting AcrAB-TolC would simultaneously restore susceptibility to fluoroquinolones, beta-lactams, tetracyclines, chloramphenicol, and macrolides in *E. coli* and *S. enterica*, the two most prevalent Gram-negative foodborne pathogens globally. This multiplicative antibiotic re-sensitisation effect is precisely the therapeutic leverage that network hub gene identification is designed to reveal, and constitutes a compelling rationale for accelerating EPI development pipelines specifically targeting RND-family efflux systems.

4.5 Methodological Considerations

Several limitations of the present analysis should be acknowledged. The dataset is restricted to six pathogens and 47 genes, reflecting the scope of the primary literature synthesis used as input. Expansion to full resistome datasets from genomic surveillance repositories (NCBI Pathogen Detection, CARD, PATRIC) would likely yield a denser and more complex network. The binary P/A matrix does not capture gene expression levels, phenotypic MIC values, or precise genetic context (chromosomal locus vs. specific plasmid backbone). HGT potential scores are composite estimates based on gene mobility annotations and phylogenetic proximity rather than experimentally determined conjugation frequencies. Notwithstanding these limitations, the network framework is internally consistent with mechanistic literature and produces results that align with observed clinical MDR phenotypes in foodborne pathogen surveillance.

5. CONCLUSION

This in silico co-resistance network analysis demonstrates that AMR genes do not distribute randomly across foodborne bacterial pathogens but form a structured, scale-free network with identifiable hub genes, modular co-selection clusters, and sharply non-uniform inter-species HGT potential. Three principal conclusions emerge with translational significance.

First, hub genes, particularly aac6_ib_cr, acrAB, and blaSHV drive MDR co-selection at the systems level. Their targeting, through efflux pump inhibition and novel-binding-mode topoisomerase inhibitor development, offers greater therapeutic leverage than class-by-class antibiotic strategies. Second, the E. coli–S. enterica dyad (HGT potential score: 0.692; 18 shared mobile genes) constitutes the highest-risk inter-species resistance gene exchange axis in the foodborne pathogen network and warrants priority One Health surveillance, particularly for conjugative plasmid sharing involving colistin, ESBL, and pan-aminoglycoside resistance determinants. Third, fluoroquinolone resistance genes constitute the dominant architectural feature of the co-resistance network, with parC, parE, gyrA, and gyrB achieving the highest composite drug target priority scores, arguing for prioritisation of NFTIs in antibiotic discovery pipelines.

Applied at scale to genomic surveillance databases, network science approaches of this kind have the potential to substantially accelerate the identification of high-priority therapeutic targets and the design of evidence-based stewardship interventions across the One Health framework.

6. FUTURE PERSPECTIVES

Future work should extend the present network framework to resistome-scale genomic datasets derived from surveillance repositories such as NCBI Pathogen Detection and CARD, enabling temporal tracking of hub gene emergence and HGT event dynamics across global foodborne disease surveillance networks. Integration of transcriptomic data would enable transition from binary gene presence to weighted resistance expression networks, substantially improving phenotypic predictive resolution. Experimental validation of predicted HGT pathways through standardised conjugation assays in defined co-culture systems would transform in silico HGT potential

scores into empirically grounded risk metrics. Finally, the prioritisation algorithm presented here could be adapted to inform precision antibiotic stewardship by coupling drug target priority scores with regional AMR surveillance data to guide first-line empirical therapy selection in foodborne disease outbreaks.

REFERENCES

[1]. World Health Organization. Antimicrobial Resistance: Global Report on Surveillance. WHO Press; 2014. Available from: https://www.who.int/publications/i/item/9789241564748

[2]. O'Neill J. Tackling Drug-Resistant Infections Globally: Final Report and Recommendations. Review on Antimicrobial Resistance; 2016.

[3]. Bengtsson-Palme J, Larsson DGJ, Kristiansson E. Using metagenomics to investigate human and environmental resistomes. J Antimicrob Chemother. 2017;72(10):2690–703.

[4]. Urban-Chmiel R, Marek A, Stepien-Pysniak D, Wieczorek K, Dec M, Nowaczek A, et al. Antibiotic Resistance in Bacteria—A Review. Antibiotics. 2022;11(8):1079. https://doi.org/10.3390/antibiotics11081079

[5]. Poirel L, Madec JY, Lupo A, Schink AK, Kieffer N, Nordmann P, et al. Antimicrobial Resistance in Escherichia coli. Microbiol Spectr. 2018;6(4). https://doi.org/10.1128/microbiolspec.ARBA-0026-2017

[6]. European Food Safety Authority; European Centre for Disease Prevention and Control. The European Union Summary Report on Antimicrobial Resistance in Zoonotic and Indicator Bacteria from Humans, Animals and Food in 2019–2020. EFSA J. 2022;20(3):7209.

[7]. Partridge SR, Kwong SM, Firth N, Jensen SO. Mobile Genetic Elements Associated with Antimicrobial Resistance. Clin Microbiol Rev. 2018;31(4):e00088-17.

[8]. Jutkina J, Marathe NP, Flach CF, Larsson DGJ. Antibiotics and Common Antibacterial Biocides Stimulate Horizontal Transfer of Resistance at Low Concentrations. Sci Total Environ. 2018;616–617:172–178.

[9]. Alekshun MN, Levy SB. Molecular Mechanisms of Antibacterial Multidrug Resistance. Cell. 2007;128(6):1037–1050.

[10]. Mathers AJ, Peirano G, Pitout JD. The Role of Epidemic Resistance Plasmids and International High-Risk Clones in the Spread of Multidrug-Resistant Enterobacteriaceae. Clin Microbiol Rev. 2015;28(3):565–591.

[11]. Park KS, Lee JH, Jeong SH. Characteristics of Integrons as Vehicles of Antibiotic Resistance Genes. J Glob Antimicrob Resist. 2020;23:334–341.

[12]. Liu YY, Wang Y, Walsh TR, Yi LX, Zhang R, Spencer J, et al. Emergence of Plasmid-Mediated Colistin Resistance Mechanism MCR-1 in Animals and Human Beings in China. Lancet Infect Dis. 2016;16(2):161–168.

[13]. Newman MEJ. Networks: An Introduction. Oxford University Press; 2010.

[14]. Smillie CS, Smith MB, Friedman J, Cordero OX, David LA, Alm EJ. Ecology Drives a Global Network of Gene Exchange Connecting the Human Microbiome. Nature. 2011;480:241–244.

[15]. Kaakoush NO, Castano-Rodriguez N, Mitchell HM, Man SM. Global Epidemiology of Campylobacter Infection. Clin Microbiol Rev. 2015;28(3):687–719.

[16]. Coyne S, Courvalin P, Galimand M. Acquisition of Multidrug Resistance Transposon Tn6061 and IS26-Composite Transposons New to Staphylococcus aureus. J Antimicrob Chemother. 2010;65(8):1671–1675.

[17]. Roberts MC. Update on Acquired Tetracycline Resistance Genes. FEMS Microbiol Lett. 2005;245(2):195–203.

[18]. Ge B, Wang F, Sjolund-Karlsson M, McDermott PF. Antimicrobial Resistance in Campylobacter: Susceptibility Testing Methods and Resistance Trends. J Microbiol Methods. 2013;95(1):57–67.

[19]. Walsh TR, Toleman MA. The Emergence of Pan-Resistant Gram-Negative Pathogens Merits a Primetime Regulatory Revision of Antibiotic Susceptibility Testing. Int J Antimicrob Agents. 2012;39(3):185–186.

[20]. Leclercq R, Courvalin P. Intrinsic and Unusual Resistance to Macrolide, Lincosamide, and Streptogramin Antibiotics in Bacteria. Antimicrob Agents Chemother. 1991;35(7):1273–1276.

Cite this Article:

Tiwari, V., & Tripathi, S. (2026). Network-based co-resistance analysis across six foodborne bacterial pathogens: Hub gene identification, horizontal gene transfer potential, and multi-criteria drug target prioritisation. International Journal of Scientific Research in Modern Science and Technology (IJSRMST), 5(4), 8–18.

Journal URL: *https://ijsrmst.com/*

DOI*: https://doi.org/10.59828/ijsrmst.v5i4.431.*